Morphological homoplasy, life history evolution, and historical biogeography of plethodontid salamanders inferred from complete mitochondrial genomes

Rachel Lockridge Mueller[1,2,3,4], J. Robert Macey[1,2], Martin Jaekel[1,2], David B. Wake[1,3], and Jeffrey L. Boore[2,3]

Keywords: plethodontid salamander, partitioned Bayesian analysis, biogeography, homoplasy, mitochondrial genomes, life history evolution

Suggested running title: Salamander mitochondrial genome phylogeny

[1] Museum of Vertebrate Zoology
3101 Valley Life Sciences Bldg.
University of California
Berkeley, CA 94720-3160

[2] Evolutionary Genomics Department
DOE Joint Genome Institute and Lawrence Berkeley National Laboratory
2800 Mitchell Dr.
Walnut Creek, CA 94598

[3] Department of Integrative Biology
3060 Valley Life Sciences Bldg.
University of California
Berkeley, CA 94720-3160

[4]To whom correspondence should be addressed

Abbreviations: bp, base pairs; MC^3, Metropolis-coupled Markov chain Monte Carlo; hLRT, hierarchical likelihood ratio test; AIC, Akaike Information Criterion; BP, Nonparametric bootstrap proportion; PP, Bayesian posterior probability; ML, maximum likelihood; MP, maximum parsimony; MLBP, maximum likelihood bootstrap proportion; MPBP, maximum parsimony bootstrap proportion; SVL, snout-vent length; dd, direct development; *Pl.*, *Plethodon*; AB, Clade A + B; PC, Clade *Plethodon* + C.

Abstract

The evolutionary history of the largest salamander family (Plethodontidae) is characterized by extreme morphological homoplasy. Analysis of the mechanisms generating such homoplasy requires an independent, molecular phylogeny. To this end, we sequenced 24 complete mitochondrial genomes (22 plethodontids and two outgroup taxa), added data for three species from GenBank, and performed partitioned and unpartitioned Bayesian, ML, and MP phylogenetic analyses. We explored four dataset partitioning strategies to account for evolutionary process heterogeneity among genes and codon positions, all of which yielded increased model likelihoods and decreased numbers of supported nodes in the topologies (PP > 0.95) relative to the unpartitioned analysis. Our phylogenetic analyses yielded congruent trees that contrast with the traditional morphology-based taxonomy; the monophyly of three out of four major groups is rejected. Reanalysis of current hypotheses in light of these new evolutionary relationships suggests that 1) a larval life history stage re-evolved from a direct-developing ancestor multiple times, 2) there is no phylogenetic support for the "Out of Appalachia" hypothesis of plethodontid origins, and 3) novel scenarios must be reconstructed for the convergent evolution of projectile tongues, reduction in toe number, and specialization for defensive tail loss. Some of these novel scenarios imply morphological transformation series that proceed in the opposite direction than was previously thought. In addition, they suggest surprising evolutionary lability in traits previously interpreted to be conservative.

Introduction

More than two-thirds of the 522 species of salamanders are members of Plethodontidae (http://amphibiaweb.org), a clade that exhibits both extreme, long-term stasis and great adaptive diversity in life history, ecology, and morphology. Morphological evolution in plethodontids is

characterized by extensive homoplasy (1). Previous studies examining the causes of this homoplasy identify recurrent morphological transformations and address both their outcomes, or derived character states, and their necessary ancestral pre-conditions (2, 3). Two plethodontid features figure prominently in shaping morphological evolution: lunglessness, a synapomorphy for the clade, and direct-development, present in three of the four major groups.

No well-supported molecular phylogenetic hypothesis exists for plethodontids. As a consequence, all analyses of morphological homoplasy are based on phylogenies constructed from many of these same homoplastic characters (4). We present a molecular phylogenetic hypothesis for plethodontids based on 27 complete mitochondrial genomes, 24 of which were sequenced for this study. We explore four strategies for partitioning our dataset in a Bayesian phylogenetic framework and compare those results to MP and ML results. Our mitochondrial phylogeny differs markedly from the morphological phylogenetic hypotheses reflected in current taxonomy; accordingly, we reevaluate plethodontid life history evolution, origins, and historical biogeography. We examine three recurring evolutionary morphological transformations: modification effecting tongue protraction, reduction in toe number, and specialization for defensive tail loss (autotomy). We present scenarios of morphological transformation that will inform future research into the evolutionary history of plethodontid form. These scenarios suggest novel transformation series for homoplastic characters. While some are consistent with traditional hypotheses regarding the direction of evolutionary change, others suggest surprising, previously unconsidered reversals in the direction of morphological evolution.

Methods

Taxon sampling. Taxa were selected to sample across plethodontid taxonomic diversity and to minimize long branches (5). The 24 taxa sequenced represent 17 of 26 plethodontid genera, all

four major plethodontid groups, and two outgroups (Figure 1). We included three complete salamander mitochondrial genomes from GenBank, which represent three additional families (NC 002756 = *Salamandra luschani*; NC 004926 = *Andrias davidianus*; NC 004021 = *Ranodon sibiricus*) (6-8).

DNA sequencing. Whole genomic DNA was extracted from frozen tissue in the Museum of Vertebrate Zoology collection. Each mitochondrial genome was PCR amplified in two to four overlapping fragments using both universal and specific primers; primer sequences are available from the authors. PCR products were sheared to ~1.5 kb with a HydroShear device (GeneMachines) and enzymatically repaired to blunt their ends. Products were gel-extracted, ligated into pUC18 vector, and electroporated into competent cells (InVitrogen) using a Gene Pulser II (BioRad). Plated cells were grown overnight. Colonies were picked using a Qbot robotic colony picker (Genetix) and processed robotically through the following steps: 1) rolling circle amplification of plasmids, 2) sequencing reactions using fluorescent dideoxynucleotide terminators, 3) clean-up, and 4) loading onto either ABI 3730XL or Megabace 4000 DNA sequencing machines. GenBank accession numbers, locality information, and alignment information are listed in supplementary material available from PNAS online.

Assembly, annotation, and alignment. Sequences from each genome were assembled into contigs using PHRAP (9) and confirmed visually using CONSED v.13 (10). Genomes were annotated manually or using DOGMA (11). Sequences of each gene were aligned using GCG v.10.3 (Accelrys) (gap creation and extension costs set to the defaults = 8 and 2, respectively), adjusted to preserve reading frame and tRNA secondary structure, and concatenated for phylogenetic analysis. Gene-by-gene alignment was necessary because of variation in gene order; these rearrangements are not informative at this phylogenetic level and will be discussed

in detail elsewhere. The control region and 1,812 other ambiguously alignable positions (including tRNA loops, beginnings and ends of many protein-coding genes, and rRNA regions with indels) were excluded, resulting in a final alignment of 14,040 bp. For one species, *Hydromantes italicus*, 384 bp were not sequenced and were coded as missing data for phylogenetic analysis.

Bayesian phylogenetic analysis. Bayesian phylogenetic analyses were implemented using MRBAYES v3.04b (12). Flat Dirichlet distributions were used for substitution rates and base frequencies, and default flat prior distributions were used for all other parameters. MC^3 analyses were run with one cold and three heated chains (temperature set to the default = 0.2) for 15 million generations and sampled every 1,000 generations. Stationarity was confirmed using CONVERGE (13) and by examining plots of -ln*L* scores and parameter values; 8-10 million generations were discarded as burn-in. The tree was rooted with the simultaneous inclusion of five outgroups: *Andrias davidianus, Ranodon sibiricus, Salamandra luschani, Ambystoma laterale,* and *Rhyacotriton variegatus*.

In addition to the unpartitioned dataset, analyses were performed using four data partitioning strategies designed to improve the fit of the substitution model to the data in light of heterogeneous nucleotide substitution processes (14, 15). The partitioning strategies divided the dataset into six, 16, 29, and 42 partitions, which will be referred to as 6p, 16p, 29p, and 42p, respectively. Each strategy included a separate partition for each ribosomal RNA and the concatenated tRNAs. Strategies differed in the partitioning of protein-coding genes: 6p defined a separate partition for all first codon positions, all second codon positions, and all third codon positions; 16p defined a separate partition for each of the 13 protein-coding genes; 29p defined a separate partition for the first and second codon positions together for each gene, and a partition

for the third codon position for each gene; and 42p defined a separate partition for each codon position in each protein-coding gene. Alternate partitioning strategies were compared using Bayes factors, the ratios of the marginal likelihoods of two alternate hypotheses (15-18). The 42p analysis was conducted using an unreleased version of MrBayes modified by J. Huelsenbeck to accommodate more than 30 data partitions.

For the unpartitioned dataset and each of the 71 total partitions used in all analyses, the best-fitting nucleotide substitution model was selected using hLRT and AIC implemented in MRMODELTEST (v.1.1b) [modified from MODELTEST, (19) by J.A.A. Nylander]. Likelihood scores were estimated on a minimum-evolution tree (ML distances) of the entire dataset. For 47 of 71 partitions, the two methods selected identical models despite AIC's penalty for increased model complexity. hLRT-selected models were used for all partitioning strategies and the unpartitioned analysis. The 42p analysis was repeated using AIC-selected models.

Comparison of Bayesian results with other phylogenetic analyses.

Equally-weighted MP and ML analyses were performed using PAUP*4.0B10 (20). MP analyses were performed both including and excluding third codon positions. Heuristic searches were performed with ten random addition replicates and TBR branch-swapping. For the ML analysis, the GTR+I+Γ and TVM+I+Γ models of nucleotide substitution and parameter values were selected using hLRT and AIC, respectively, implemented in MODELTEST V3.06 (19). Both were used in heuristic searches with five random addition replicates. BP for clades were assessed for MP analyses (1000 pseudo-replicates) and ML analyses (100 pseudo-replicates). ML analysis of amino acids was performed using quartet puzzling implemented in TREE-PUZZLE 5.0 (21). The mtREV24 substitution model was used with Γ-distributed rates, with amino acid frequencies and α estimated from the data.

Statistical test of the monophyly of traditional taxonomic groups. To test whether all possible topologies containing the traditional taxonomic groups Plethodontinae, Hemidactyliini, Plethodontini, or Bolitoglossini are statistically rejected by our Bayesian analyses of mitochondrial genomes, the 95% credible set of trees for each of the four partitioned analyses and the unpartitioned analysis was constructed (14, 22, 23). This is the set of all topologies contained in the cumulative 0.95 posterior probability distribution. All topologies within these sets were examined for the presence of a monophyletic Plethodontinae, Hemidactyliini, Plethodontini, or Bolitoglossini.

Results

Comparisons of different analyses and partitioning strategies. The results of all ML analyses and the MP analysis excluding third codon positions are largely consistent with the partitioned Bayesian results, although MP and amino acid ML produce phylogenies with fewer resolved nodes. MP analysis with third codon positions included yields a different topology.

All partitioned Bayesian analyses result in increased model likelihoods relative to the unpartitioned analysis, but PP of two nodes in the topologies drops below 0.95. The unpartitioned analysis supports sister group relationships between "Bolitoglossa sp. nov." and "Thorius sp. nov." (PP = 0.97) and between *Hydromantes* and *Aneides* (PP = 0.99); no partitioned analysis supports these nodes with PP > 0.95. Analyses of the 6p, 16p, 29p, and 42p partitioning strategies yield near-identical topologies and nodal support, although model likelihood scores differ significantly based on Bayes factor comparisons (Table 1). The 42p analyses using models selected with AIC or hLRT yield the same topology and nodal support.

Plethodontid phylogenetic hypothesis. The results of the partitioned Bayesian and ML nucleotide analyses, and the MP analysis excluding third codon positions, are shown in Figure 2.

The monophyly of Plethodontidae is supported by all analyses (PP and BP = 1.0). Three previously unnamed clades are identified as follows: Clade A = *Gyrinophilus porphyriticus, Pseudotriton ruber, Stereochilus marginatus* and *Eurycea bislineata*; Clade B = *Oedipina poelzi, Nototriton abscondens,* "Bolitoglossa sp. nov.," "Thorius sp. nov.," *Batrachoseps attenuatus, Batrachoseps wrightorum,* and *Hemidactylium scutatum;* and Clade C = *Desmognathus wrighti, Desmognathus fuscus, Phaeognathus hubrichti, Hydromantes brunus, Hydromantes italicus, Ensatina eschscholtzii, Aneides hardii,* and *Aneides flavipunctatus*. This topology is presented because it results from model-based analyses, appropriate for this dataset which displays saturation, long terminal branches, and short internodes (24, 25). In the MP analysis including third codon positions, *H. scutatum* is sister to all other plethodontids (BP = 0.89), Clade A is sister to Clade C (BP = 0.56), and "Bolitoglossa sp. nov." is sister to "Thorius sp. nov." (BP = 1.0) (not shown). *Hemidactylium scutatum* is never sister to *Batrachoseps* in additional parsimony analyses and is consistently located at the base of the plethodontid tree (BP = <0.50 – 0.99) (not shown).

Traditionally recognized plethodontid groups

Desmognathinae and Plethodontinae. The traditional basal dichotomy within plethodontids separates the subfamilies Desmognathinae and Plethodontinae (Figure 1). Monophyly of Desmognathinae *(D. wrighti, D. fuscus, P. hubrichti)* is supported (PP and MLBP = 1.0); however, the group is nested within Clade C. Monophyly of Plethodontinae is rejected.

Hemidactyliini. Monophyly of Hemidactyliini is rejected. *Hemidactylium scutatum* is sister to *Batrachoseps* in Clade B. The remaining hemidactyliine lineages form Clade A.

Plethodontini. Monophyly of Plethodontini is rejected. The plethodonine lineages *(P. cinereus, P. petraeus, P. elongatus, E. eschscholtzii, A. hardii,* and *A. flavipunctatus)* are paraphyletic with respect to the desmognathines and *Hydromantes*.

Bolitoglossini. Monophyly of Bolitoglossini is rejected, although each of the three clades comprising it is supported (PP and MLBP = 1.0). The tropical plethodontids (*O. poelzi, N. abscondens,* "Bolitoglossa sp. nov.," and "Thorius sp. nov.") are sister to a clade comprised of *Batrachoseps* and *H. scutatum*. *Hydromantes* is a member of Clade C. The basal relationships within Clade C and the position of "Bolitoglossa sp. nov." within the tropical plethodontids are not supported with PP > 0.95.

Relationships among salamander families. Our mitochondrial phylogeny supports a sister-group relationship between Salamandridae *(S. luschani)* and Ambystomatidae *(A. laterale)* and between Cryptobranchidae *(A. davidianus)* and Hynobiidae *(R. sibiricus)* (PP and MLBP ≥ 0.99), assuming the root does not fall within either of these two relationships. Similarly, a sister-group relationship between these two clades, to the exclusion of Rhyacotritonidae *(R. variegatus),* is supported (PP and MLBP = 1.0). Because inter-familial relationships among salamanders remain unresolved, we present our phylogeny rooted along an internal node with a basal polytomy; however, rooting with Crytobranchidae + Hynobiidae supports a sister-group relationship between Rhyacotritonidae and Plethodontidae (PP and MLBP = 1.0) (not shown) (26).

Statistical test of the monophyly of traditional taxonomic groups. The number of topologies in the 95% credible sets ranged from three to 11 for each Bayesian analysis. In all cases, the topologies differed only in the position of "Bolitoglossa sp. nov." within the tropical salamanders, or in the relationships within Clade C, both of which are not supported with PP > 0.95 in our phylogeny. None of the topologies in the 95% credible sets contained a monophyletic

Plethodontinae, Hemidactyliini, Bolitoglossini, or Plethodontini; therefore, the monophyly of these taxonomic groups is rejected statistically.

Discussion

Different levels of nodal support among partitioning strategies and analyses. The higher model likelihood scores of the partitioned analyses relative to the unpartitioned analysis indicate that the data are better explained by partitioning the dataset than by applying an average model and parameter values across all genes and codon positions (14, 15). Partitioned analyses yield two fewer nodes with PP > 0.95 than the unpartitioned analysis, suggesting that the high support for these nodes in the unpartitioned analysis may result from model mis-specification (27, 28). Partitioning by codon position across the 13 protein-coding genes (6p) is significantly better than partitioning by gene (16p), although it defines fewer partitions.

The most striking results of our phylogenetic analyses are: 1) the inclusion of *Hydromantes* in Clade C + *Plethodon,* 2) the inclusion of the desmognathines in Clade C + *Plethodon*, and 3) the inclusion of *H. scutatum* in Clade B. The first two are supported by PP and MLBP = 1.0, and the third is supported by PP = 1.0 and MLBP = 0.89.

Life History Evolution. Plethodontids exhibit several life history strategies: some species hatch as aquatic larvae and metamorphose into terrestrial or semi-aquatic adults; some retain larval morphology throughout ontogeny; and some are direct developers, hatching from terrestrial eggs as miniature adults. Direct development in salamanders is unique to plethodontids, which suggests a biphasic ancestral life history that includes an aquatic larval stage and metamorphosis. The morphological plethodontid phylogeny (29) implied two appearances of direct development—at the base of Bolitoglossini + Plethodontini, and in nested lineages in Desmognathinae—and no instances of the re-evolution of a larval stage. Later, a desmognathine

mtDNA phylogeny suggested the surprising basal position of direct development and subsequent re-evolution of larvae in derived lineages, consistent with three total evolutionary transitions in plethodontid life history strategy (30). Three different transitions had been inferred by Wake (1), but all were from a biphasic life history to direct development. Our results indicate higher levels of homoplasy in life history evolution, necessitating a minimum of four transitions. Figure 3 shows three different, equally parsimonious life history evolution scenarios. Discrimination among these scenarios will require weighting either the loss or re-evolution of larvae in Clades A and B. However, all of these scenarios necessitate at least one instance of a larval stage re-evolving from a direct-developing ancestor, a morphological transformation rarely reported and previously considered to be unlikely (31). A direct-developing plethodontid ancestor (Figure 3a) necessitates reevaluation of several hypotheses including a stream origin for the clade and the ecological causes of lung loss (32-38).

Morphological Homoplasy

Tongue Evolution--Because plethodontids are lungless, the tongue musculoskeletal elements used for ventilation in lunged salamanders are freed from this functional constraint. Consequently, these elements are specialized for tongue protraction (1). Direct-developing lineages are freed from an additional constraint; they no longer require the tongue skeleton for larval suction feeding, a function that may conflict with specialization for extreme tongue protraction (39). Three categories of tongue function are recognized: protrusible, attached projectile, and free. All recent phylogenetic hypotheses for plethodontids require extensive convergence such that none of these tongue types defines a monophyletic group, and different morphological modifications effecting free tongue protraction have evolved in different lineages.

Convergence in tongue function represents repeated morphological exploration within different lineages made possible by loss of an ancestral functional constraint (2, 40).

Protrusible tongues are the least modified from the ancestral state. To effect protraction, force is applied by the paired m. subarcualis rectus I to the epibranchials and transmitted via ceratobranchial I to the basibranchial element in the tongue pad; all of these elements are cartilaginous and comprise the hyobranchial apparatus, or tongue skeleton (Figure 4). The tongue skeleton folds slightly during protrusion, and the tongue can extend ~7% SVL beyond the mouth (41, 42). The anterior tip of the tongue is tightly attached to the front of the lower jaw by paired, short genioglossus muscles.

Attached projectile tongues are specialized for directionality and distance, extending ~15% SVL beyond the mouth (41). The anterior tip is attached by elongated genioglossus muscles whose insertions have moved posteriorly along the lower jaw. Epibranchial length is increased relative to the other elements, and ceratobranchial lengths are decreased. The tongue skeleton folds significantly during projection. Various changes to the associated musculoskeletal components are present.

Free tongues are specialized for extreme long-distance projection, and the muscular connection between the tongue tip and lower jaw has been lost. Morphological modifications are similar to those seen in attached projectile tongues, but tongues are projected 30-80% SVL (43). In two independent cases, projection is truly ballistic--the tongue skeleton leaves the mouth altogether, and the tongue reaches the prey under its own momentum (44, 45).

Free-tongued lineages are characterized by one of two force-transmitting mechanisms to effect tongue projection. The first [“Option 1” (40)] is mechanically similar to protrusible tongue protraction. The second (“Option 2”) differs in that ceratobranchial II, rather than ceratobranchial

I, is the force-transmitting pathway from the epibranchials to the basibranchial; this difference significantly alters projection biomechanics. Commitment by a lineage to Option 1 or Option 2 may be irreversible, because an evolutionary transition between the two requires an intermediate tongue skeletal configuration less optimal for tongue projection than either option (40).

The simplest scenario for convergent tongue evolution consistent with our phylogeny requires five total transitions among functional types, similar to the number implied by the morphological phylogeny. Based on comparisons with outgroups, the ancestral state for plethodontids is a protrusible tongue. Free tongues appear three times: at the base of Clade A, at the base of the tropical plethodontids, and in *Hydromantes*. Attached projectile tongues appear twice: at the base of *Batrachoseps* + *H. scutatum*, and in *Ensatina*. The morphological transformation series in this scenario are similar to those suggested by the morphological phylogeny.

Such extensive functional mode homoplasy is expected of lineages exploring a finite set of morphological possibilities (2, 3); the mitochondrial phylogeny is consistent with this interpretation of convergent tongue evolution. However, our finding that *Batrachoseps, Hydromantes,* and the tropical plethodontids do not form a monophyletic Bolitoglossini demonstrates extensive homoplasy of characters previously thought to have evolved more conservatively (29). Despite their different tongue functional categories, these three groups share many morphological modifications for tongue protraction including: the loss of two different skeletal elements and one muscle, the fusion of several skeletal elements, changes in the proportions of the tongue skeletal elements, Option 2 force-transmission and the associated changes in relative size and orientation of additional tongue skeletal elements, loss of a cell type in the motor column of the neck and trunk, and possession of a complex musculoskeletal aiming

cylinder to control tongue direction (29). Based on the mitochondrial phylogeny, all of these characters either 1) evolved three times in parallel, or 2) evolved twice in parallel and were regained or reversed in *H. scutatum*. Again, choosing between these scenarios will require weighting certain morphological transformations; however, in either case, our results necessitate multiple gains and losses of morphological characters not previously thought to be homoplastic.

Toe Loss--A reduction from five to four toes characterizes four plethodontid taxa: *Hemidactylium scutatum, Eurycea quadridigitata, E. chamberlaini,* and *Batrachoseps*. Traditional phylogenetic hypotheses imply at least three independent losses, resulting from a developmental constraint imposed by decreasing limb bud size and large cell size (3). The sister group relationship between *Batrachoseps* and *H. scutatum* in the mitochondrial phylogeny decreases the minimum number of toe reductions from three to two.

Tail Autotomy--Plethodontids vary in their degree of specialization for defensive tail loss. Some lineages have highly specialized tail morphologies in which shortened vertebrae and musculature, and weakened connective tissue, form a constriction at the base of the tail and localize inter-vertebral breakage ("constricted-based tails"). In addition, the skin breaks one vertebra behind the muscle, forming a sleeve over the wound that facilitates healing, blastema formation, and subsequent tail regeneration ("wound-healing") (46). Other lineages possess wound-healing, but do not localize breakage to the base of their uniformly slender tails ("slender-based tails"). Finally, some lineages have no specializations for loss; their tails simply break mechanically. These thick, often laterally compressed tails are used for aquatic propulsion ("thick-based tails"). Most lineages comprising the two traditional basal clades, Desmognathinae and Hemidactyliini, are aquatic or semi-aquatic with thick-based tails. Close outgroups also lack autotomy, which implies an unspecialized plethodontid ancestral tail morphology. Wound-

healing was inferred to have arisen in the common ancestor of Plethodontini and Bolitoglossini, following evolution of direct development, and was interpreted as a necessary pre-condition for convergent and parallel evolution of constricted- and slender-based tails (46). Tail loss specialization coincident with a shift from aquatic to terrestrial habitat was also noted, to a lesser extent, within desmognathines and hemidactyliines.

We outline a substantially different scenario for the evolution of tail autotomy. We infer the evolution of wound-healing in the ancestral plethodontid, because it is present in multiple lineages spanning the basal mitochondrial dichotomy. Across the two main clades, AB and PC, convergent evolution of all three tail types is present: constricted-based tails appear in the tropical plethodontids and *H. scutatum* (AB), and in *E. eschscholtzii* (PC); slender-based tails appear in *Batrachoseps* and secondarily in several tropical lineages (AB), and in *Plethodon* and non-arboreal *Aneides* (PC); thick-based tails appear in Clade A (AB), and in the desmognathines (PC). In this scenario, the presence of thick-based tails indicates a loss of wound-healing specialization and a new reliance on the tail for aquatic propulsion. Within these largely aquatic groups with thick-based tails, however, there are terrestrial lineages; this terrestriality is associated with the re-evolution of a novel, less efficient tail autotomy specialization that differs from the ancestral specialization. A similar loss of wound-healing specialization has occurred in some non-aquatic species as well. Within PC, *Hydromantes* and some *Aneides* evolved reliance on their tails for terrestrial and arboreal locomotion, respectively, and tail loss is generally infrequent in these clades. In this scenario for the evolution of tail autotomy, morphological change from one tail type to another proceeds in previously unconsidered directions. Surprisingly, lineages with specializations for autotomy have, in some instances, given rise to lineages with a generalized tail morphology more typical of basal forms.

Plethodontid origins and historical biogeography. Wilder and Dunn first proposed an Appalachian center of origin for plethodontids in 1920 (32). That view is still widely accepted and is supported by three factors: 1) high present-day plethodontid adaptive diversity and species richness in the Appalachians (47); 2) current Appalachian distributions of the basal groups Desmognathinae and Hemidactyliini, whereas nested clades have both eastern and western North American distributions (Plethodontini), western North American and European distributions (*Hydromantes* and *Batrachoseps,* clade Bolitoglossini), or Central and South American distributions (the tropical plethodontids, clade Bolitoglossini); and 3) existence of Appalachian mountain streams, the inferred ancestral habitat, since the postulated origin of the clade in the Cretaceous [(1, 32, 34), but see (37, 38)].

The "Out of Appalachia" hypothesis does not receive phylogenetic support from our analysis, although we cannot refute it. The basal split in the mitochondrial phylogeny is into two clades, each of which contains both eastern and western lineages, and we report many novel associations between eastern and western groups. Our results, coupled with the current plethodontid distribution and that of *Rhyacotriton,* imply a North American origin of the clade with expansion into Europe and Central and South America; however, the current species distributions do not retain any signal that reflects the early biogeographic history of this ancient group within geologically and climatically dynamic North America. Fossil evidence dates back only to the Miocene, when *Aneides, Plethodon,* and *Batrachoseps* are found in Western North America, and *Hydromantes* is found in Slovakia (48-50).

Conclusions. We present the phylogenetic relationships among 27 plethodontid and outgroup mitochondrial genomes. Our results are surprising; we do not recover three of the four major groups currently recognized. Analyses of complete mitochondrial genomes have been used to

resolve the relationships among lineages in other ancient groups, yielding both expected and unexpected phylogenies [e.g. ratites (51), insects (52), teleosts (53), and hexapods (54)]. Both methodological limitations and biological processes can cause gene trees to differ from species trees (55-57). We advocate the use of multiple, independent genetic markers for taxonomic revision and look forward to forthcoming nuclear data; if these mitochondrial genome results are corroborated, retention of some taxonomic group names will be possible, although the lineages contained within the new clades will change. Consideration of multiple markers will lead to a more complete understanding of the history of Plethodontidae. In addition, it will teach us about the different processes that have shaped the evolutionary histories of the genetic markers themselves. Finally, it will instruct future researchers on the strengths and weaknesses of different datasets and analytical approaches in reconstructing relationships among ancient lineages.

Acknowledgements. We thank M. Fourcade, J. Keuhl, and D. Engle for technical assistance; D. Hillis, T. Reeder, A. Leaché, M. Mahoney, E. Rosenblum, V. Vredenburg, and M. Wake for comments on the manuscript; M. Brandley for discussion; J. Huelsenbeck for modifications to MrBayes; and A. Seago for the larva in Fig. 3. Part of this work was performed by the U. of California Lawrence Berkeley National Lab under the auspices of the U.S. Dept. of Energy, Office of Biological and Environmental Research, contract No. DE-AC03-76SF00098. RLM was supported by an NSF predoctoral fellowship and NIH training grant. Additional funds came from an NSF doctoral dissertation improvement grant to RLM and DBW and the AmphibiaTree Project (NSF EF-0334939).

1. Wake, D. B. (1966) *Memoirs of the Southern California Academy of Sciences* **4,** 1-111.
2. Wake, D. B. & Larson, A. (1987) *Science* **238,** 42-48.
3. Wake, D. B. (1991) *Am. Nat.* **138,** 543-567.
4. Wake, D. B. (1993) *Herpetologica* **49,** 229-237.
5. Hillis, D. M. (1998) *Sys. Biol.* **47,** 3-8.
6. Zhang, P., Chen, Y.-Q., Zhou, H., Wang, X.-L. & Qu, L.-H. (2003) *Mol. Phylogenet. Evol.* **28,** 620-626.
7. Zhang, P., Chen, Y.-Q., Liu, Y.-F., Zhou, H. & Qu, L.-H. (2003) *Gene***,** 93-98.
8. Zardoya, R., Malaga-Trillo, E., Veith, M. & Meyer, A. (2003) *Gene* **317,** 17-27.
9. Green, P. (1994).
10. Gordon, D., Abajian, C. & Green, P. (1998) *Genome Res.* **8,** 195-202.
11. Wyman, S. K., Jansen, R.K., and J.L. Boore (2004) *Bioinformatics* **in press**.
12. Huelsenbeck, J. P. & Ronquist, F. (2001) *Bioinformatics* **17,** 754-755.
13. Warren, D. L., Wilgenbusch, J. & Swofford, D. L. (2003).
14. Nylander, J. A. A., Ronquist, F., Huelsenbeck, J. P. & Nieves-Aldrey, J. L. (2004) *Sys. Biol.* **53,** 47-67.
15. Brandley, M. B., Schmitz, A. & Reeder, T. W. (2005) *Sys. Biol.* **in press**.
16. Lavine, M. & Schervish, M. J. (1999) *Am. Stat.* **53,** 119-122.
17. Huelsenbeck, J. P. & Imennov, N. S. (2002) *Sys. Biol.* **51,** 155-165.
18. Kass, R. E. & Raftery, A. E. (1995) *J. Am. Stat. Assoc.* **90,** 773-795.
19. Posada, D. & Crandall, K. A. (1998) *Bioinformatics* **14,** 817-818.
20. Swofford, D. L. (1998) (Sinauer Associates, Sunderland, MA).
21. Schmidt, H. A., Strimmer, K., Vingron, M. & von Haeseler, A. (2000).
22. Reeder, T. W. (2003) *Mol. Phylogenet. Evol.* **27,** 384-397.
23. Buckley, T. R. (2002) *Sys. Biol.* **51,** 509-523.
24. Sullivan, J. & Swofford, D. L. (1997) *J. Mamm. Evol.* **4,** 77-86.
25. Felsenstein, J. (2004) *Inferring phylogenies* (Sinauer Associates Inc., 23 Plumtree Road, P. O. Box 407, Sunderland, MA, 01375.
26. Larson, A. & Dimmick, W. W. (1993) *Herp. Monogr.* **7,** 77-93.
27. Suzuki, Y., Glazko, G. V. & Nei, M. (2002) *Proc. Natl. Acad. Sci. U. S. A.* **99,** 16138-16143.
28. Erixon, P., Svennblad, B., Britton, T. & Oxelman, B. (2003) *Sys. Biol.* **52,** 665-673.
29. Lombard, R. E. & Wake, D. B. (1986) *Syst. Zool.* **35,** 532-551.
30. Titus, T. A. & Larson, A. (1996) *Sys. Biol.* **45,** 451-472.
31. Duellman, W. E. & Hillis, D. M. (1987) *Herpetologica* **43,** 141-173.
32. Wilder, I. W. & Dunn, E. R. (1920) *Copeia* **1920,** 63-68.
33. Noble, G. K. (1925) *J. Morphol. Physiol.* **40,** 341-416.
34. Beachy, C. K. & Bruce, R. C. (1992) *Am. Nat.* **139,** 839-847.
35. Dunn, E. R. (1928) *Am. Nat.* **62,** 236-248.
36. Dunn, E. R. (1926) *Salamanders of the Family Plethodontidae* (Smith College, Northampton, Massachusetts).
37. Ruben, J. A., Reagan, N. L., Verrell, P. A. & Boucot, A. J. (1993) *Am. Nat.* **142,** 1038-1051.
38. Ruben, J. A. & Boucot, A. J. (1989) *Am. Nat.* **134,** 161-169.
39. Deban, S. M. & Marks, S. B. (2002) *Zool. J. Linn. Soc.* **134,** 375-400.

40. Wake, D. B. (1982) in *Environmental Adaptation and Evolution*, eds. Mossakowski, D. & Roth, G. (Gustav Fischer, Stuttgart, New York), pp. 51-66.
41. Larsen, J. H. J., Beneski, J. T. J. & Wake, D. B. (1989) *J. Exp. Zool.* **252,** 25-33.
42. Lombard, R. E. & Wake, D. B. (1977) *J. Morphol.* **153,** 39-80.
43. Wake, D. B. & Deban, S. M. (2000) in *Feeding: Form, Function, Phylogeny*, ed. Schwenk, K. (Academic Press, San Diego, CA), pp. 95-116.
44. Deban, S. M., Wake, D. B. & Roth, G. (1997) *Nature* **389,** 27-28.
45. Deban, S. M., O'Reilly, J. C. & Nishikawa, K. C. (2001) *Am. Zool.* **41,** 1280-1298.
46. Wake, D. B. & Dresner, I. G. (1967) *J. Morphol.* **122,** 265-306.
47. Wake, D. B. (1987) *Annals of the Missouri Botanical Garden* **74,** 242-264.
48. Tihen, J. A. & Wake, D. B. (1981) *J. Herp.* **15,** 35-40.
49. Clark, J. M. (1985) *J. Herp.* **19,** 41-47.
50. Venczel, M. & Sanchiz, B. (2004) *Amphibia Reptilia* **in press**.
51. Cooper, A., Lalueza-Fox, C., Anderson, S., Rambaut, A., Austin, J. & Ward, R. (2001) *Nature* **409,** 704-707.
52. Stewart, J. B. & Beckenbach, A. T. (2003) *Mol. Phylogenet. Evol.* **26,** 513-526.
53. Miya, M., Takeshima, H., Endo, H., Ishiguro, N. B., Inoue, J. G., Mukai, T., Satoh, T. P., Yamaguchi, M., Kawaguchi, A., Mabuchi, K., Shirai, S. M. & Nishida, M. (2003) *Mol. Phylogenet. Evol.* **26,** 121-138.
54. Nardi, F., Spinsanti, G., Boore, J. L., Carapelli, A., Dallai, R. & Frati, F. (2003) *Science* **299,** 1887-1889.
55. Pamilo, P. & Nei, M. (1988) *Mol. Biol. Evol.* **5,** 568-583.
56. Maddison, W. P. (1997) *Sys. Biol.* **46,** 523-536.
57. Ballard, J. W. O. & Whitlock, M. C. (2004) *Mol. Ecol.* **13,** 729-744.

Figure 1. Taxa sequenced grouped according to traditional plethodontid clades. Hemidactyliini+Bolitoglossini+Plethodontini = Plethodontinae. Plethodontinae + Desmognathinae = Plethodontidae.

Figure 2. Consensus phylogram inferred using partitioned Bayesian analysis of 27 complete mitochondrial genomes (42 data partitions). Numbers above the internodes are PP. Numbers below the internodes are BP; upper numbers are MLBP using AIC-selected models, and lower numbers are MPBP excluding 3rd positions. -- indicates relationships not resolved, or resolved differently, by an analysis. ML and MP analyses recover "Bolitoglossa sp. nov." + "Thorius sp. nov." (BP = 0.74 and 0.95, respectively). Shapes indicate traditional taxonomic groups. Open circles = Desmognathinae, open squares = Bolitoglossini, closed squares = Hemidactyliini, closed circles = Plethodontini. Open squares + closed squares + closed circles = Plethodontinae. Species lacking shapes are outgroup taxa; families are indicated in parentheses. "" indicates unnamed species. A, B, and C designate novel clades referred to in the text.

Figure 3. Three equally parsimonious reconstructions of life history evolution on a simplified mitochondrial genome cladogram. Larvae represent transitions from direct-development to a biphasic life history that includes a larval stage. "dd" represents transitions from a biphasic life history to direct development. 3a. The ancestral plethodontid evolves direct development. Larvae re-evolve three times: at the base of Clade A, in *H. scutatum* (Clade B), and in *D. fuscus* (Clade C). 3b. The ancestral plethodontid has a biphasic life history. Direct development evolves at the base of Clade B and at the base of Clade *Pl.* + C. Larvae re-evolve in *H. scutatum* (Clade B) and *D. fuscus* (Clade C). 3c. The ancestral plethodontid has a biphasic life history. Direct

development evolves twice within Clade B--at the base of the tropical plethodontids and in *Batrachoseps*--and at the base of Clade C + *Pl*. Larvae re-evolve in *D. fuscus* (Clade C).

Figure 4. The hyobranchial apparatus, or tongue skeleton, of a plethodontid salamander with a protrusible tongue *(Desmognathus quadramaculatus)*. The basibranchial element is in the tip of the tongue.

Table 1: Pairwise $2\log_e$ Bayes Factor comparisons among partitioning strategies. Values >10 indicate "very strong" evidence in favor of the more likely partitioning strategy over the alternate (18). The marginal likelihoods of the unpartitioned analysis and the partitioning strategies, in order of highest to lowest likelihood, are: 42p = -184,509.32; 29p = -185,318.50; 6p = -186,047.49; 16p = -187,846.57; unpartitioned = -189,363.71.

Table 2 (online supplementary material): List of specimens sequenced for the study, Museum of Vertebrate Zoology (MVZ) catalogue numbers, locality information, GenBank accession numbers, and TreeBASE accession number.

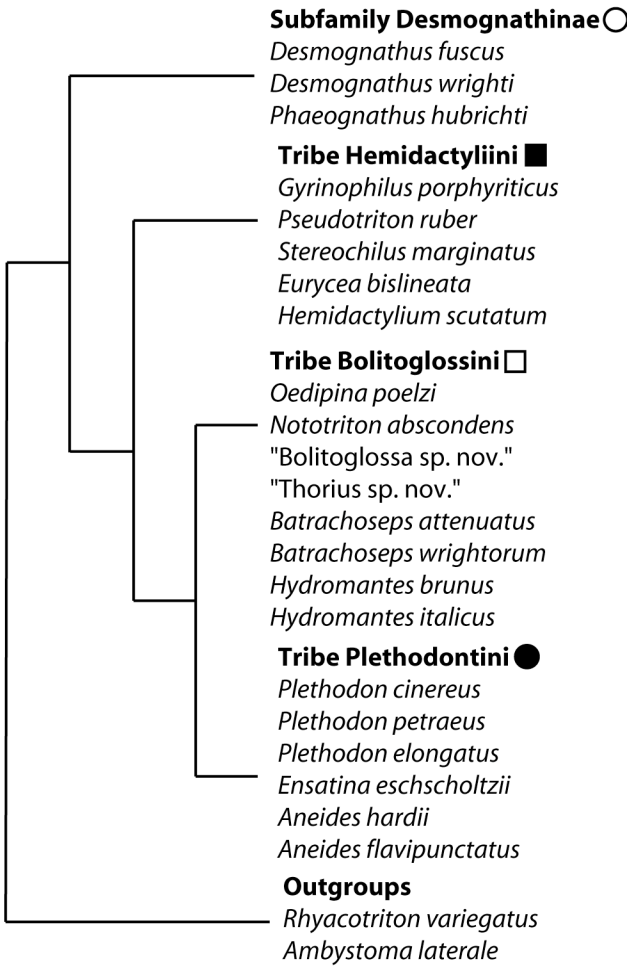
Subfamily Desmognathinae ○
Desmognathus fuscus
Desmognathus wrighti
Phaeognathus hubrichti
Tribe Hemidactyliini ■
Gyrinophilus porphyriticus
Pseudotriton ruber
Stereochilus marginatus
Eurycea bislineata
Hemidactylium scutatum
Tribe Bolitoglossini □
Oedipina poelzi
Nototriton abscondens
"Bolitoglossa sp. nov."
"Thorius sp. nov."
Batrachoseps attenuatus
Batrachoseps wrightorum
Hydromantes brunus
Hydromantes italicus
Tribe Plethodontini ●
Plethodon cinereus
Plethodon petraeus
Plethodon elongatus
Ensatina eschscholtzii
Aneides hardii
Aneides flavipunctatus
Outgroups
Rhyacotriton variegatus
Ambystoma laterale

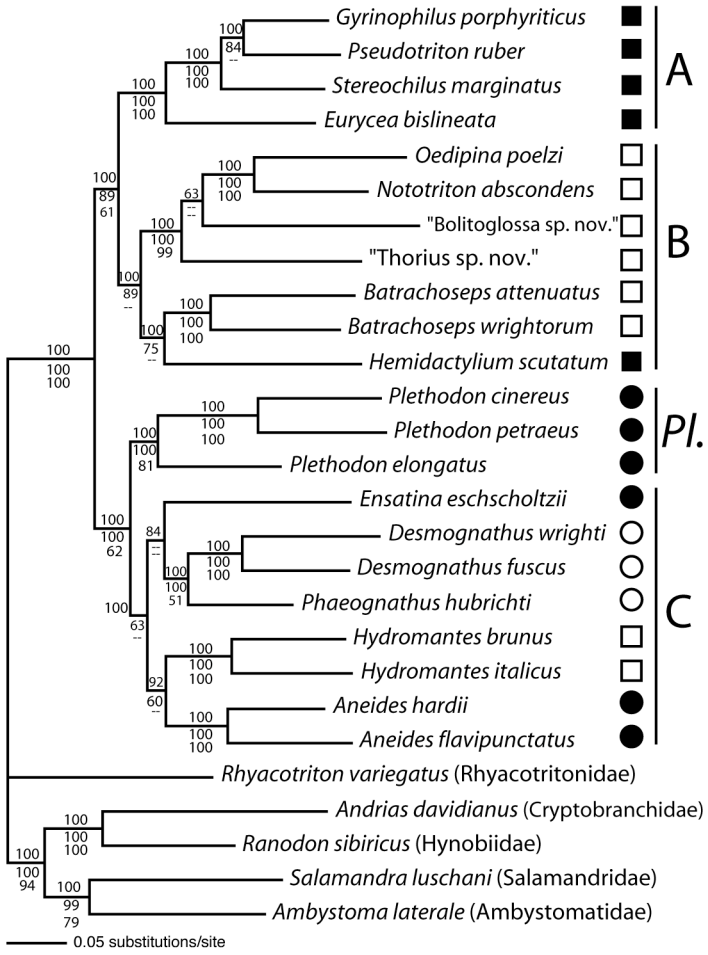
Gyrinophilus porphyriticus
Pseudotriton ruber
Stereochilus marginatus
Eurycea bislineata
A
Oedipina poelzi
Nototriton abscondens
"Bolitoglossa sp. nov."
"Thorius sp. nov."
Batrachoseps attenuatus
Batrachoseps wrightorum
Hemidactylium scutatum
B
Plethodon cinereus
Plethodon petraeus
Plethodon elongatus
Pl.
Ensatina eschscholtzii
Desmognathus wrighti
Desmognathus fuscus
Phaeognathus hubrichti
Hydromantes brunus
Hydromantes italicus
Aneides hardii
Aneides flavipunctatus
C
Rhyacotriton variegatus (Rhyacotritonidae)
Andrias davidianus (Cryptobranchidae)
Ranodon sibiricus (Hynobiidae)
Salamandra luschani (Salamandridae)
Ambystoma laterale (Ambystomatidae)
0.05 substitutions/site

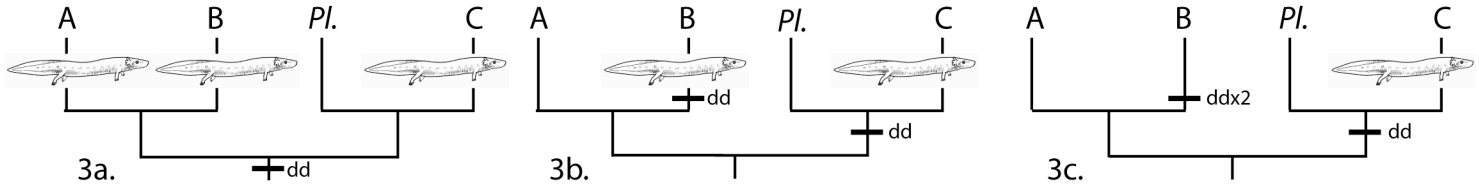
A
B
Pl.
C
dd
3a.
A
B
Pl.
C
dd
dd
3b.
A
B
Pl.
C
ddx2
dd
3c.

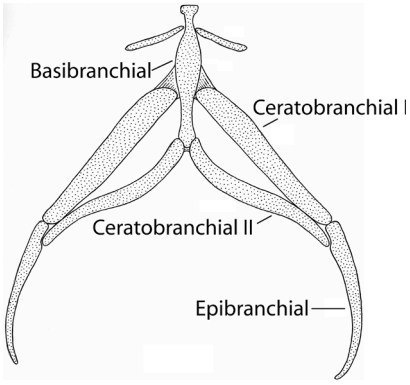
Basibranchial
Ceratobranchial I
Ceratobranchial II
Epibranchial

	42p	29p	6p	16p	Unpart.
Unpart.	9708.78	8090.42	6632.44	3034.28	-
16p	6674.5	5056.14	3598.16	-	-
6p	3076.34	1457.98	-	-	-
29p	1618.36	-	-	-	-
42p	-	-	-	-	-

Taxon Name	MVZ Number
Nototriton abscondens	203743
Oedipina poelzi	207128
Bolitoglossa sp. nov.	225875
Thorius sp. nov.	231444
Batrachoseps wrightorum	224902
Batrachoseps attenuatus	230761
Hydromantes brunus	230641
Hydromantes italicus	163996
Aneides flavipunctatus	219973
Aneides hardii	226110
Plethodon cinereus	225101
Plethodon elongatus	220003
Plethodon petraeus	222650
Ensatina eschscholtzii	236229
Eurycea bislineata	225074
Gyrinophilus porphyriticus	173504
Hemidactylium scutatum	225077
Pseudotriton ruber	220897
Stereochilus marginatus	233227
Phaeognathus hubrichti	173507
Desmognathus fuscus	224931
Desmognathus wrighti	222618
Ambystoma laterale	173468
Rhyacotriton variegatus	222581

Locality Information
1.5 km N Poasito junction on road to Varablanca; elevation 1950 m; Prov. Heredia, Costa Rica
Carril Bosque Eterno, N of Pantanoso Trail, Monteverde Reserve; elevation 1595 m Prov. Alajuela, Costa Rica
Aquaduct Trail along Rio Coton, below Las Tablas, Prov. Puntarenas, Costa Rica
Mexican Hwy. 175, 4.2 mi N Suchixtepec; elevation 8860 ft; Oaxaca, Mexico
U.S. Forest Service 2231, 1.8 mi E junction Hwy. 46; Marion Co., Oregon, United States
Winchuck River Rd. at Winchuck Campground; elevation 150 ft; Curry Co., Oregon, United States
0.6 mi NE (by road) Briceburg; Mariposa Co., California, United States; TRS: T4S R18E Sec. 2 SW 1/4
Mine shaft in Upper Fabiano Valley, 2 km W and 2.6 km S La Spezia; elevation 400 m Liguria Region, Italy
Green Riffle, 4.4 mi N Siskiyou County line on Hwy.96; Siskiyou Co., California, United States
Lincoln National Forest, County Hwy. 6563, ca. 11 mi S by Air and 3 mi W by Air, Cloudcroft, Otero Co., New Mexico, United States
State Game Lands No. 122, Centerville Rd.; Crawford Co., Pennsylvania, United States
Miller Redwood Company property, Site 3 along Rock Creek Rd.; Del Norte Co., California, United States
Crocker-Pigeon Mt. Wildlife Mgmt. area, 1.5-1.9 mi W Chamberlain Rd., SW Lafayette; elevation 360-460 m; Walker Co., Georgia, United States
0.4 mi E Sonoma Co. Line on Hwy 12, Napa Co., California, United States
Hauger Rd., ca. 0.2-0.5 mi W junction Four Mile Run Rd., vicinity Donegal; Westmoreland Co., Pennsylvania, United States
South Mts., Spring on County Rte. 1969, 5.5 mi SE junction of 1969 and Hwy. 64, Burke Co., North Carolina, United States
Clarence Fahnestack State Park, vicinity Pelton Pond Natural Area; Putnam Co., New York, United States
Foreman Rd., near Hwy. 64, Highlands; Macon Co., North Carolina, United States
Neuse River campground, ca. 5 mi N Havelock; Craven Co., North Carolina, United States
3 mi NW McKenzie on U.S. Rte. 31, Butler Co., Alabama, United States
S. Shelbourne Rd., Smead Brook, vicinity Greenfield; Franklin Co., Massachusetts, United States
Roan Gardens, Pisgah National Forest; elevation 6200 ft; Mitchell Co., North Carolina, United States
Rainbarrel Slough, Cook Co., Illinois, United States
17 mi Sign on Clark Rd., off 10 mi River Hall Rd., NE Fort Bragg; Mendocino Co., California, United States

GenBank Accession Numbers	Alignment available from TreeBASE
	http://www.treebase.org/treebase/
	Accession Number:

This work was performed under the auspices of the US Department of Energy's Office of Science, Biological and Environmental Research Program and by the University of California, Lawrence Livermore National Laboratory under Contract No. W-7405-Eng-48, Lawrence Berkeley National Laboratory under contract No. DE-AC03-76SF00098 and Los Alamos National Laboratory under contract No. W-7405-ENG-36.